Progress In Electromagnetics Research C, Vol. 54, 117–124, 2014

Dual-band Circularly Polarized Deformed Monopole Antenna

Huan Zhang*, Yong Chang Jiao, Wei Long Liang, and Liang Lu

Abstract—A novel dual-band circularly polarized monopole antenna fed by coplanar waveguide (CPW) is proposed. Deformed monopole and asymmetrical ground are utilized to achieve dual-band characteristic, by adjusting the tuning stub close to the deformed monopole, the antenna performance can be further improved. Measured results show that the proposed antenna has an impedance bandwidth of 1.44 GHz centered at 3.42 GHz for the lower band and 400 MHz centered at 5.2 GHz for the upper band, and the 3-dB axial ratio bandwidth is 900 MHz centered at 3.25 GHz and 400 MHz centered at 5.1 GHz respectively. The measured results agree well with the simulated results.

1. INTRODUCTION

In recent years, CPW-fed circularly polarized antenna has received considerable attention for its simpler fabrication and easy integration with integrated circuit [1, 2]. In addition, multiband antenna is usually desired in certain cases to avoid out-of-band interference. For the inherent advantages of immunity to the multipath propagation and depolarization effects such as mismatch between transmitter and receiver, circularly polarized antenna is becoming more and more popular in various wireless communications to enhance system performance. The CP feature can be obtained when two orthogonal modes with equal amplitude but in phase quadrature are excited.

Many techniques have been proposed in recent years to achieve dual-band circularly polarized antenna. Two parallel deformed monopoles fed by CPW are used in [3] to obtain dual band CP antenna with low frequency ratio and wide bandwidths. Micro-strip feed line with tuning stub can also be used to obtain dual-band CP antenna [4]. In [5], C-shape grounded strip and slots around two opposite corners are utilized to design a dual-band dual-sense circularly polarized antenna; a monopole antenna with a ground plane embedded with an inverted-L slit is propose in [6] to achieve dual-band circular polarization, two bands of width 150 MHz centered at 2.5 GHz and 230 MHz centered at 3.4 GHz are obtained. However, the antennas mentioned above are either complex in structure or narrow in axial-ratio bandwidth. In [7], a monopole antenna is designed to achieve both linear and circular polarization, but it has only one AR band.

In this paper, a novel dual-band circularly polarized deformed monopole antenna is presented. The antenna is mainly comprised of three structures: asymmetrical ground, deformed monopole and a tuning stub close to the monopole, the asymmetrical ground and monopole are used to achieve dual-band circular polarization while the tuning stub is for the improvement of the antenna performance. Simulated results shown that the impedance bandwidth is 40% (2.6–3.9 GHz, 3.25 GHz) and 8% (4.85–5.25 GHz, 5.05 GHz), and the AR bandwidth is 27.7% (2.8–3.7 GHz, 3.25 GHz) for the lower band and 5.8% (5–5.3 GHz, 5.15 GHz) for the upper band.

Received 6 October 2014, Accepted 22 October 2014, Scheduled 28 October 2014
* Corresponding author: Huan Zhang (zhmfpp@163.com).
The authors are with the National Key Laboratory of Antennas and Microwave Technology, Xidian University, Xi'an, Shaanxi 710071, People's Republic of China.

2. DESIGN OF THE PROPOSED ANTENNA

Figure 1 shows the fabrication of the designed dual-band circularly polarized monopole antenna. It is printed on an FR4 substrate with a dimension of $50 \times 50 \times 0.8\,\text{mm}^3$, a relative permittivity $\varepsilon_r = 4.4$ and a loss tangent $\tan\theta = 0.02$. The antenna is fed by a $50\,\Omega$ CPW having a feed-line of width 4 mm and two identical gaps of width 0.35 mm. Two small slots in the feed-line are designed to improve the impedance matching as well as the AR bandwidth. Other dimensions are shown in Figure 1 with unit millimeters.

The dual-band CP feature is mainly related to the deformed monopole with width W and asymmetrical ground which is first proposed in [1] to achieve circular polarization. A tuning stub with length L is added close to the deformed monopole to further improve the performance of the proposed antenna. The antenna shown in Figure 1 will produce right- and left-hand circularly polarized (RHCP and LHCP) radiations in the $+z$ and $-z$ directions respectively.

3. ANALYSIS AND DISCUSSION

In this paper, the antenna is simulated and optimized using the Ansoft High Frequency Structure Simulator (HFSS) ver.15 based on the finite element method (FEM). Parameters sensitive to the design are optimized and the realization of dual-band feature are clarified in this section, during this process, all other parameters not mentioned stay constant as shown in Figure 1.

3.1. Mechanism of the Dual-Band Circular Polarization

The dual-band performance of the proposed antenna can be explained by Figure 2. It is clearly shown that two resonance modes are produced in the designed antenna. At lower frequency, stronger current exits where coupling between signal strip and asymmetric ground is strong, at upper frequencies, owing

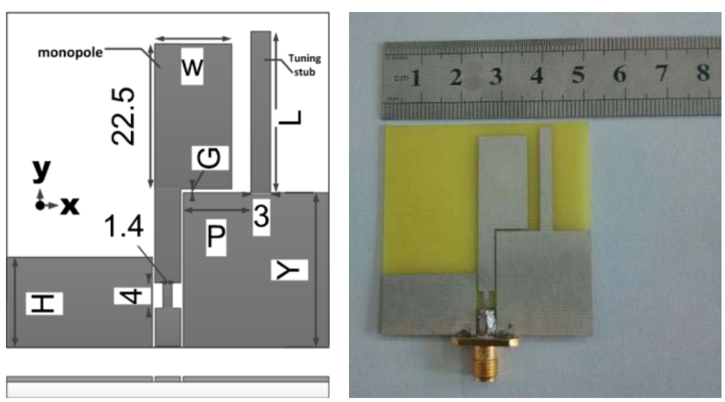

Figure 1. Antenna configuration.

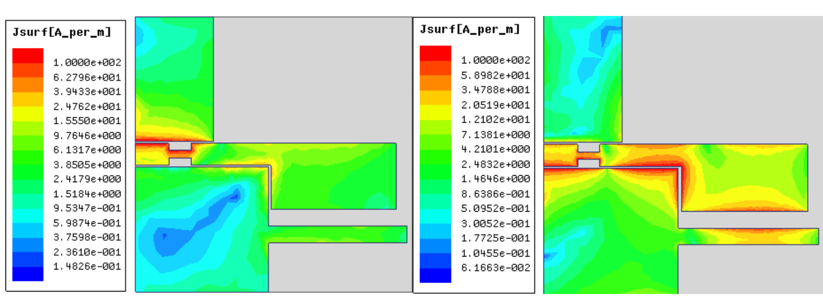

(a) (b)

Figure 2. Current distribution at (a) 3.3 GHz and (b) 5.1 GHz.

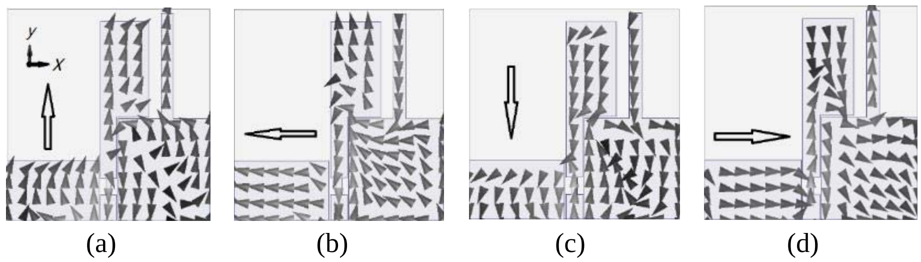

Figure 3. Simulated surface vector current distribution of proposed antenna at 3.3 GHz for four phases, (a) 0°, (b) 90°, (c) 180°, (d) 270°.

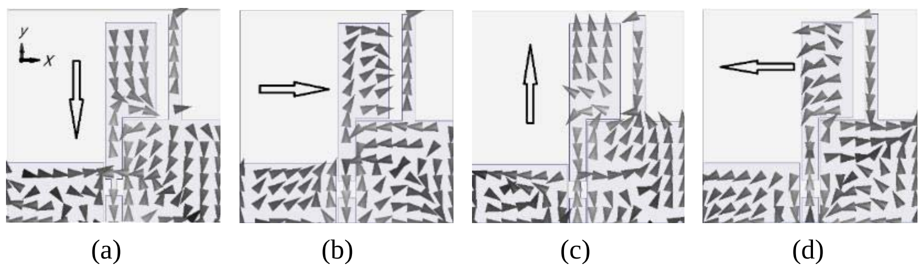

Figure 4. Simulated surface vector current distribution of proposed antenna at 5.1 GHz for four phases, (a) 0°, (b) 90°, (c) 180°, (d) 270°.

to the adding of the deformed monopole, a strong coupling between the monopole and ground occurs, which leads to another operation band.

Figure 3 and Figure 4 show the vector current distributions of the proposed antenna at 3.3 GHz and 5.1 GHz viewed from the $+z$ direction respectively, four different current phases from 0° to 270° with interval 90° is presented. The 0° phase reference at lower frequency of 3.3 GHz shows that the dominant radiating current are $+y$ direction in the asymmetrical ground plane, for the 90° phase, it shows the dominant current are in $-x$ direction. In other words, after one quarter-period, the vector current at 3.3 GHz rotates in the right-hand direction by 90° in the $+z$ direction, which satisfies the requirement of the spatial and temporal quadrature for circular polarization.

For the current distribution at upper frequency of 5.1 GHz shown in Figure 4, it is shown that the dominant current are in $-y$ direction for the 0° phase in the monopole structure and $+x$ direction for the 90° phase, this also meets the condition for circular polarization that two or more orthogonal linearly polarized modes, of equal amplitude and 90° phase difference, are independently excited. It can also be concluded from Figure 3 and Figure 4 that the asymmetrical ground is responsible for the circular polarization at lower frequency while the deformed monopole is related to the circular polarization performance at upper frequency.

3.2. Effect of the Deformed Monopole (W and G)

Based on the analysis of the surface vector current of the proposed antenna, the variation of W changes the size of the deformed monopole which is related to the circular polarization at upper frequencies. Then the effects of the width of the deformed monopole are given out in Figure 5 and Figure 6. From Figure 5, it can be seen that, as W increases, the impedance bandwidth at upper band shifts toward lower frequency while the impedance bandwidth at lower frequency almost stay the same. This is due to the weak current on the monopole. Figure 6 shows the variation of AR with different W, it shows clearly that the axial ratio at upper frequency changes a lot as W changes while the axial ratio at lower frequency nearly keep constant. This also demonstrates that the deformed monopole is responsible for the circular polarization at upper frequencies.

The gap between the deformed monopole and the ground plane is also studied to make the design process clear. As G increases from 0.5 mm to 1.5 mm, the two resonant frequencies at lower frequency

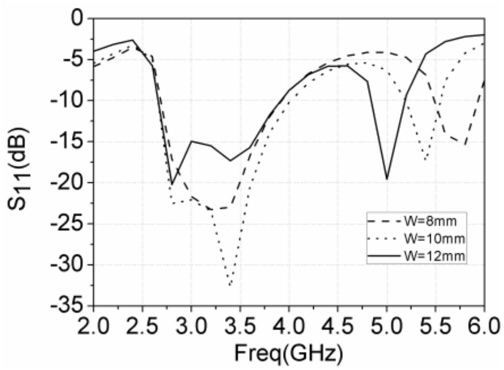

Figure 5. Simulated S_{11} with varying W.

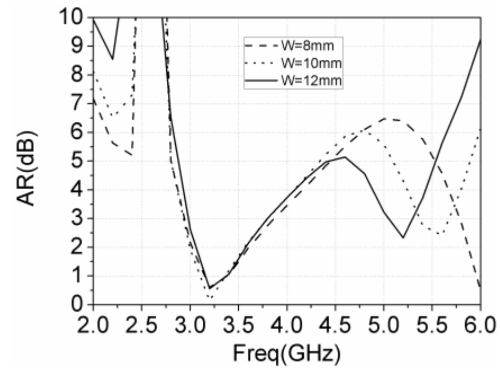

Figure 6. Simulated AR with varying W.

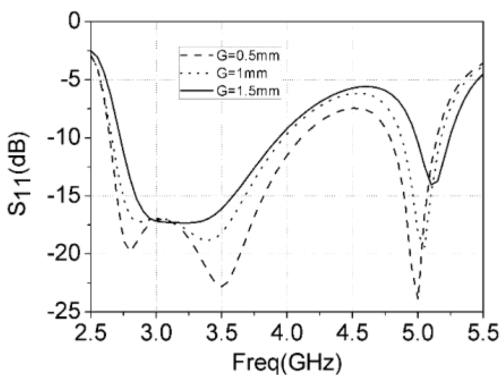

Figure 7. Simulated S_{11} with varying G.

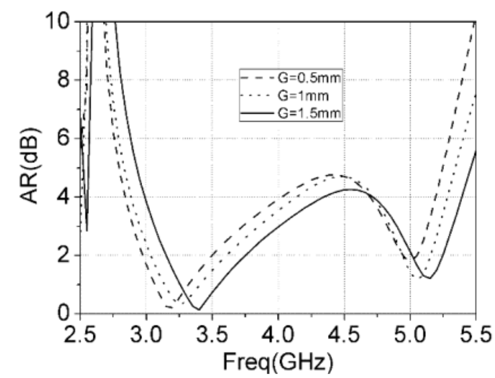

Figure 8. Simulated AR with varying G.

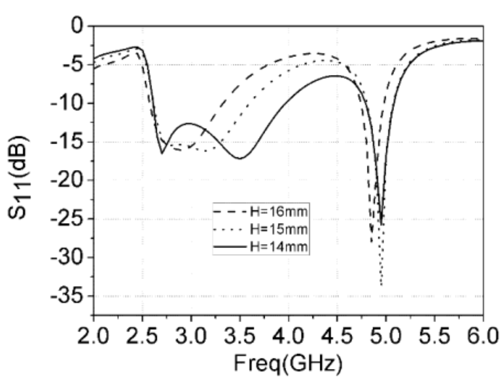

Figure 9. Simulated S_{11} with varying H.

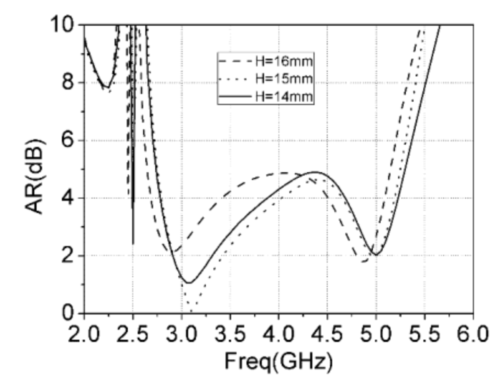

Figure 10. Simulated AR with varying H.

incorporate, leading to a narrow band. And both the two 3-dB AR bands shift to upper frequency as G increases.

3.3. Effect of the Asymmetrical Ground (H and Y)

The effect of the size of the ground plane on both sides of the feed-line is analyzed. It can be seen in Figure 9 and Figure 11 that H and Y, i.e., the dimensions of the asymmetrical ground in y direction, has a greater influence on the return loss at lower frequencies. As H decreases or Y increases, two resonant frequency points occurs around 2.6 GHz and 3.5 GHz, which usually means an enhancement of the impedance bandwidth. From Figure 10 and Figure 12, we can see that the AR performance at

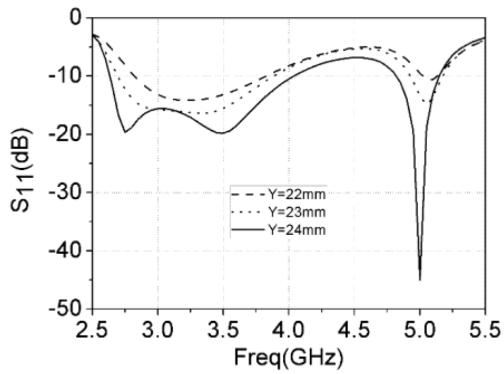

Figure 11. Simulated S_{11} with varying Y.

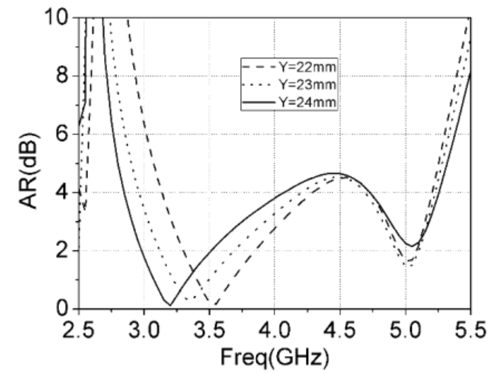

Figure 12. Simulated AR with varying Y.

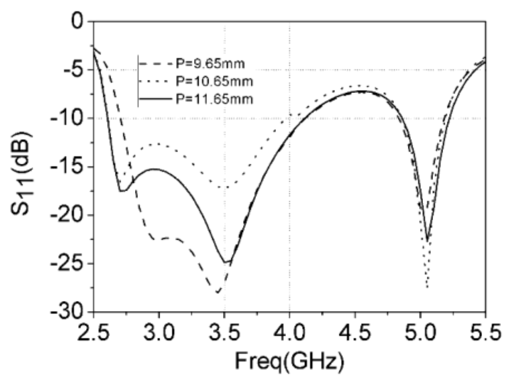

Figure 13. Simulated S_{11} with varying P.

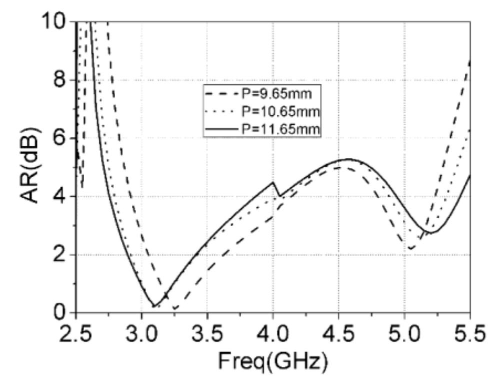

Figure 14. Simulated AR with varying P.

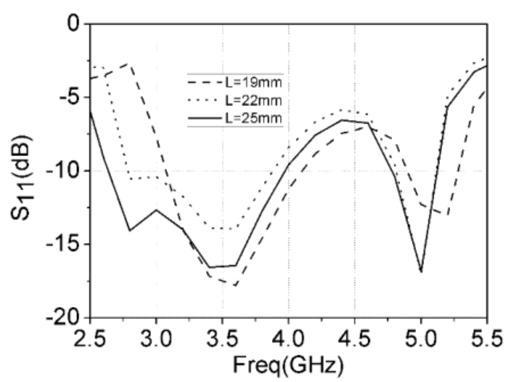

Figure 15. Simulated S_{11} with varying L.

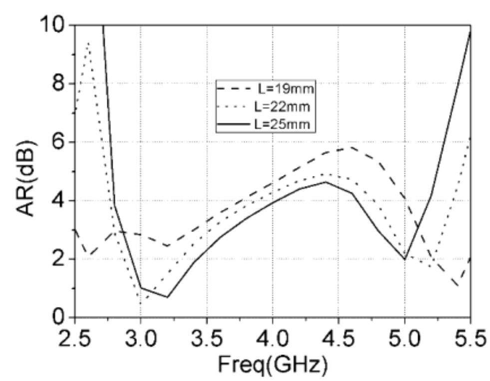

Figure 16. Simulated AR with varying L.

lower frequencies changes greater than that at upper frequencies as H and Y changes, a slight shift of the AR to the lower frequency can be noted as Y increases. The results shown in Figures 7–10 can be concluded that the CP characteristics at lower frequencies of the proposed antenna is mainly related to the asymmetrical ground, which agrees with the conclusion obtained in Section 3.1.

3.4. Effect of the Tuning Stub (P and L)

In order to make the 10-dB impedance bandwidth coincide with the 3-dB AR bandwidth and extend the antenna to a good performance, a tuning stub is added close to the deformed monopole to improve the antenna performance, Figure 13 and Figure 14 reveal the influence of the location of the tuning stub on the designed antenna. As it can be seen that the 3-dB AR band around 5 GHz shifts slightly with the change of the stub position, thus by choosing proper value for the parameter P, broader CP bandwidth in higher frequencies can be obtained. Figure 15 shows the variation of simulated S_{11} with varying L, it shows that the S_{11} varies little as L ranges from 19 mm to 25 mm, but as to the variation of 3-dB AR shown in Figure 16, as L increases, the resonant frequency for lower band shifts to upper band while the resonant frequency for upper band shifts to lower band. Through extensive optimizations, it is found that 25 mm for L is a better choice.

4. RESULTS AND COMPARISON

Based on the studies in previous sections, the dual-band circularly polarized deformed monopole antenna proposed in this paper is designed with sensitive parameters shown in Table 1. The antenna is successfully implemented and measured. Figure 17 and Figure 18 show the measured 10-dB return

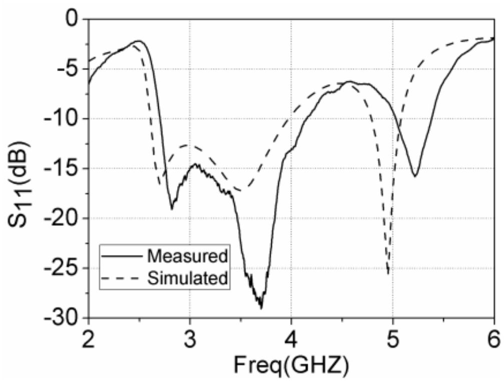

Figure 17. Simulated and measured S_{11}.

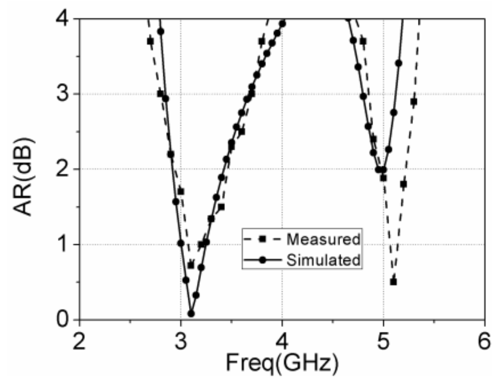

Figure 18. Simulated and measured AR.

Table 1. Antenna parameters (unit: mm).

Parameters	H	Y	L	P	W	G
Value	14	24	25	10.65	12	0.5

Table 2. Comparison of published antennas.

	Impedance Bandwidth	3-dB AR Bandwidth	Antenna Size (mm)
[3]	1.45–1.72 GHz (17% 1.585 GHz) 1.86–2.29 GHz (21% 2.075 GHz)	1.47–1.61 GHz (9% 1.54 GHz) 1.87–2.09 GHz (11.1% 1.98 GHz)	$70 \times 70 \times 1.6$
[6]	2.17–8.47 GHz (118.4% 5.32 GHz)	2.41–2.55 GHz (5.6% 2.48 GHz) 3.45–4.35 GHz (23.1% 3.9 GHz)	$40 \times 39 \times 1.6$
[8]	1.83–3.23 GHz (55.33% 2.53 GHz) 4.99–6.16 GHz (20.98% 5.575 GHz)	1.88–2.6 GHz (6.25% 2.24 GHz) 4.95–6.8 GHz (31.49% 5.875 GHz)	$50 \times 50 \times 1.6$
This work	2.7–4.14 GHz (42% 3.42 GHz) 5–5.4 GHz (7.7% 5.2 GHz)	2.8–3.7 GHz (32.14% 3.25 GHz) 4.9–5.3 GHz (7.8% 5.1 GHz)	$50 \times 50 \times 0.8$

loss bandwidth and 3-dB AR bandwidth respectively. It shows the proposed antenna has an impedance bandwidth 2.7–4.14 GHz for the lower band and 5–5.4 GHz for the upper band with two 3-dB AR bands 2.8–3.7 GHz and 4.9–5.3 GHz respectively. Then the effective AR bands are 900 MHz centered at 3.25 GHz and 300 MHz centered at 5.15 GHz. The measured AR agrees well with the simulated results while the measured S_{11} shifts to higher frequencies, this is mainly due to the fabrication error and imperfect testing environment. A comparison of the proposed antenna with published work is made in term of size, 10-dB impedance bandwidth and 3-dB AR bandwidth with results presented in Table 2. The results show that the antenna in this paper is either simple in structure or good in performance, it is also of practical use in WiMAX application. Figure 19 and Figure 20 show the simulated and measured radiation patterns at 3.1 GHz and 5.1 GHz respectively, and Figure 21 shows the gain of the proposed antenna in $+z$ direction, note the proposed antenna radiates RHCP in $+z$ direction and LHCP in $-z$ direction.

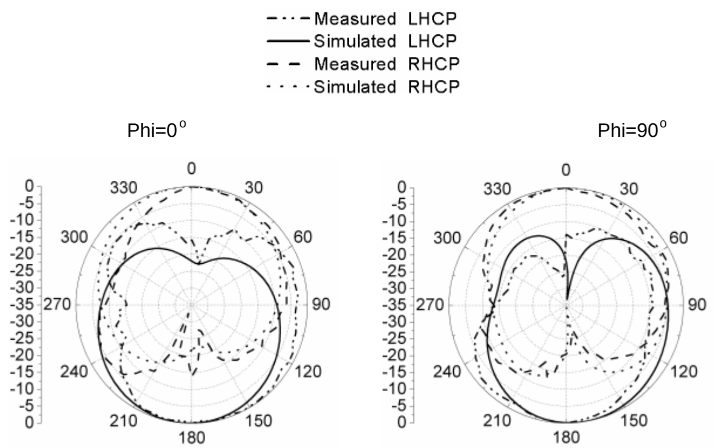

Figure 19. Simulated and measured radiation patterns at 3.1 GHz.

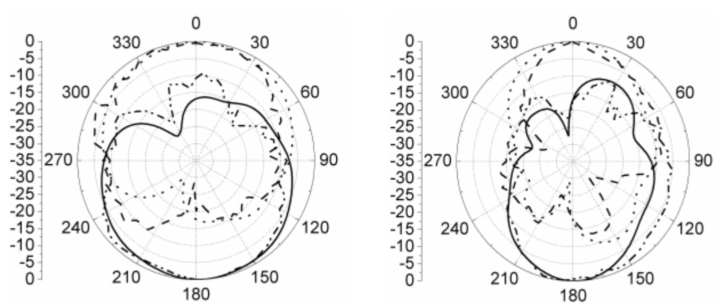

Figure 20. Simulated and measured radiation patterns at 5.1 GHz.

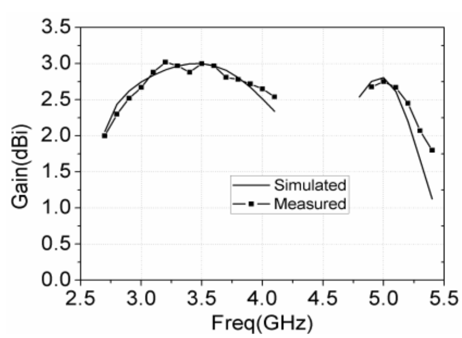

Figure 21. Simulated and measured gain in $+z$ direction.

5. CONCLUSION

A dual-band circularly polarized deformed monopole antenna is proposed in this paper. By introducing the asymmetrical ground and a deformed monopole, two CP band can be obtained. Analysis of the antenna shows that the deformed monopole is responsible for the circular polarization at higher frequencies while the CP at lower frequencies is mainly related to the asymmetrical ground. A tuning stub close to the monopole is introduced as a micro-controller to further improve the antenna performance. Measured results show the impedance bandwidth are 1.44 GHz centered at 3.42 GHz and 400 MHz centered at 5.2 GHz, and that the 3-dB AR bandwidth are 900 MHz centered at 3.25 GHz and 400 MHz centered at 5.1 GHz.

REFERENCES

1. Jan, J. Y., C. Y. Pan, K. Y. Chiu, and H. M. Chen, "Broadband CPW-fed circularly-polarized slot antenna with an open slot," *IEEE Trans. Antennas Propag.*, Vol. 61, No. 3, 1418–1422, Mar. 2013.
2. Felegari, N., J. Nourinia, C. Ghobadi, and J. Pourahmadazar, "Broadband CPW-fed circularly polarized square slot antenna with three inverted-L-shape ground strips," *IEEE Antennas Wireless Propag. Lett.*, Vol. 10, 274–277, Apr. 2011.
3. Yung, E. K. N. and C.-H.Chen, "Dual-band circularly-polarized CPW-fed slot antenna with a small frequency ratio and wide bandwidths," *IEEE Trans. Antennas Propag.*, Vol. 59, No. 4, 1379–1384, Apr. 2011.
4. Esfandiarpour, S., H. R. Hassani, and A. Frotanpour, "A dual-band circularly polarized monopole antenna for WLAN application," *2011 Proc. 5th EUCAP*, 346–349, 2011.
5. Chen, Y. Y., Y. C. Jiao, G. Zhao, F. Zhang, Z. L. Liao, and Y. Tian, "Dual-band dual-sense circularly polarized slot antenna with a C-shaped grounded strip," *IEEE Antennas Wireless Propag. Lett.*, Vol. 10, 915–918, 2011.
6. Christiina, F. J., J.-W. Wu, and C.-J. Wang, "Novel broadband monopole antennas with dual-band circular polarization," *IEEE Trans. Antennas Propag.*, Vol. 57, No. 4, 1027–1034, Apr. 2009.
7. Wand, C. J. and Y. C. Lin, "New CPW-fed monopole antennas with both linear and circular polarisations," *IET Microw. Antennas Propag.*, Vol. 2, No. 5, 466–472, 2008.
8. Weng, W.-C., J.-Y. Sze, and C.-F. Chen, "A dual-broadband circularly polarized slot antenna for WLAN application," *IEEE Trans. Antennas Propag.*, Vol. 62, No. 5, 2837–2841, May 2014.